The Clustering of Telomeres and Colocalization with Rap1, Sir3, and Sir4 Proteins in Wild-Type *Saccharomyces cerevisiae*

Monica Gotta,* Thierry Laroche,* Andrea Formenton,* Laurent Maillet,§ Harry Scherthan,‡ and Susan M. Gasser*

*Swiss Institute for Experimental Cancer Research, CH-1066 Epalinges/Lausanne, Switzerland; ‡Department of Human Genetics, Universität Kaiserslauten, D-67663 Kaiserslauten, Federal Republic of Germany; and §Ecole Normale Supérieure de Lyon, 46, Allée d'Italie F-69364 Lyon, France

Abstract. We have developed a novel technique for combined immunofluorescence/in situ hybridization on fixed budding yeast cells that maintains the three-dimensional structure of the nucleus as monitored by focal sections of cells labeled with fluorescent probes and by staining with a nuclear pore antibody. Within the resolution of these immunodetection techniques, we show that proteins encoded by the *SIR3*, *SIR4*, and *RAP1* genes colocalize in a statistically significant manner with Y' telomere-associated DNA sequences. In wild-type cells the Y' in situ hybridization signals can be resolved by light microscopy into fewer than ten foci per diploid nucleus. This suggests that telomeres are clustered in vegetatively growing cells, and that proteins essential for telomeric silencing are concentrated at their sites of action, i.e., at telomeres and/or subtelomeric regions. As observed for Rap1, the Sir4p staining is diffuse in a *sir3⁻* strain, and similarly, Sir3p staining is no longer punctate in a *sir4⁻* strain, although the derivatized Y' probe continues to label discrete sites in these strains. Nonetheless, the Y' FISH is altered in a qualitative manner in *sir3* and *sir4* mutant strains, consistent with the previously reported phenotypes of shortened telomeric repeats and loss of telomeric silencing.

S EVERAL lines of evidence, including in situ hybridization with whole chromosome probes, suggest that the organization of chromosomes within the interphase nucleus is not random (for review see Cremer et al., 1993). Indeed, it is generally assumed that three-dimensional nuclear organization is likely to facilitate essential nuclear functions, such as transcription, the processing and transport of mRNA, replication, and recombination. Evidence for the organization of chromosomes in prophase nuclei was provided over a hundred years ago by Rabl's observation that salamander chromosomes are positioned in nuclei with centromeres clustered at one pole and the telomeres at the opposite pole (Rabl, 1885). Work by Sedat and his colleagues later lent support to this notion through the study of the polytene salivary gland chromosomes of *Drosophila melanogaster*. They found that centromeres, fused into the chromocenter, abut the nuclear envelope within a restricted area while telomeres tended to cluster at the opposite pole (Mathog et al., 1984; Hochstrasser et al., 1986). A peripheral localization of telomeres has been also reported in *Trypanosoma* (Chung et al., 1990), in plant cells (Shaw et al., 1992), and in vegetatively growing fission yeast (Funabiki et al., 1993), although in mammalian cultured cells this is clearly not the case (Vourc'h et al., 1993). Electron micrographs show, on the other hand, that the dark staining, inactive heterochromatin of differentiated mammalian cells (Rae and Franke, 1972), as well as the inactive X chromosome (Walker et al., 1991), often occupy zones near the nuclear periphery.

In budding yeast the essential, abundant nuclear protein, Repressor Activator Protein 1 (Rap1[1]; Shore and Nasmyth, 1987) binds multiple sites within the $(TG_{1-3})_n$ sequence at the ends of yeast telomeres, as well as many internal chromosomal sites, where it plays roles both in the transactivation of abundant, constitutively expressed transcripts, and in the repression of the silent mating type loci (for review see Gilson and Gasser, 1995). We have previously shown by immunofluorescence techniques that anti-Rap1 antibodies stain brightly the ends of all the chromosomes in a pachytene nuclear spread (Klein et al., 1992), confirming genetic and biochemical results that suggested a biological role for Rap1 in telomere maintenance (Conrad et al., 1990; Lustig et al., 1990; Wright et al., 1992).

---

1. *Abbreviations used in this paper:* DIG, digoxigenin; FISH, fluorescence in situ hybridization; IF, immunofluorescence; Rap1, repressor activator protein 1.

Both immunofluorescence and immunoelectron micros-
copy studies also reveal intense anti-Rap1 staining in a
limited number of foci in interphase nuclei of diploid yeast
cells (6–8 per nucleus; Klein et al., 1992; Palladino et al.,
1993a; Cockell et al., 1995). Assuming that the Rap1 stain-
ing reflects yeast telomeric DNA, this would indicate that
the 64 telomeres are clustered together in groups of
roughly 8. Quantitation of the immunoelectron micros-
copy shows that over 70% of these clusters of Rap1 stain-
ing are found within a peripheral zone measuring one fifth
of the nuclear radius, which comprises 50% of the spheri-
cal nuclear volume. On the other hand, smaller signals
from the silver-enhanced immunogold labeling, presum-
ably reflecting individual molecules of Rap1, are distrib-
uted in an apparently random fashion throughout the nu-
cleus (Klein et al., 1992).

The localization of Rap1 in large foci is intriguing be-
cause telomeres are sites of a Rap1-dependent chromatin-
mediated gene repression in yeast (Gottschling et al.,
1990). This repression reflects a telomere-proximal posi-
tion effect and shares many characteristics with the repres-
sion conferred on genes positioned near centromeric het-
erochromatin in flies, which is clustered in the so-called
chromocenter (for review see Sandell and Zakian, 1992).
The focal Rap1 staining pattern is disrupted in a number
of mutants that affect telomere proximal silencing, namely
those deficient for *SIR3, SIR4*, for histone NH_2-termini,
and two *rap1* alleles that encode truncated forms of the
protein, *rap1-21* and *rap1-17* (Palladino et al., 1993a;
Cockell et al., 1995; Hecht et al., 1995). We have recently
shown that antibodies recognizing the two histone-binding
proteins, Silent Information Regulators 3 and 4 (Sir3p and
Sir4p; Hecht et al., 1995), both of which are essential for
chromatin-mediated repression, reveal a focal staining
pattern like that observed with anti-Rap1 (Palladino et al.,
1993a; Cockell et al., 1995). As of yet, however, no direct
colocalization of the proteins with telomeres has been
demonstrated.

The observation that immunologically detectable Rap1
foci are lost concomitantly with the loss of telomeric re-
peats in the yeast mutant *est1* (Ever Shorter Telomeres 1,
Lundblad and Szostak, 1989), supports the interpretation
that the foci detected by anti-Rap1 antibodies reflect the
numerous Rap1 molecules bound to telomeric DNA (Pal-
ladino et al., 1993a). Since both the Rap1 and Sir3p focal
patterns of immunostaining are delocalized in the histone
and *sir* mutants when telomeric silencing is abolished (Pal-
ladino et al., 1993a, Cockell et al., 1995, Hecht et al., 1995),
it became pertinent to ask whether under these conditions
Rap1 and Sir proteins are displaced from telomeric DNA.
Alternatively, telomeres themselves might have a dis-
persed subnuclear distribution. To distinguish between
these two possibilities, a technique that would permit the
simultaneous detection of proteins and DNA with the
greatest possible resolution was required. Although elec-
tron microscopy is optimal for high resolution immunolo-
calization (see Klein et al., 1992), the detection of specific
DNA sequences is not yet feasible on embedded yeast
cells. Confocal microscopy with fluorescently labeled
probes, on the other hand, is readily adapted to both im-
munolocalization and in situ hybridization techniques
(e.g., Ekwall et al., 1995). Although the limit of resolution

imposed by laser microscopy techniques (estimated at 200
nm) is significant in a small organism like *S. cerevisiae*,
yeast provides the possibility to correlate staining patterns
with functional states by analysis in mutant strains.

We present here a novel double-labeling technique for
S. cerevisiae using specific probes for subtelomeric in situ
hybridization and antibodies recognizing either Rap1,
Sir3p, or Sir4p. Confocal sectioning and image reconstruc-
tion, as well as the staining of nuclear pores, allows us to
monitor the nuclear morphology. We show that in struc-
turally preserved wild-type cells over 70% of the foci de-
tected by FISH using a subtelomeric probe colocalize with
Rap1 and Sir4p foci and 54% with Sir3p foci. This sup-
ports genetic evidence suggesting that these proteins func-
tion largely at telomeres. Intriguingly, Sir4p is delocalized
in a *sir3⁻* strain, and Sir3p is delocalized in a *sir4⁻* strain;
in both *sir⁻* strains, Rap1 staining no longer predomi-
nantly colocalizes with telomeric DNA. Consistent with
the idea that the loss of Sir proteins and Rap1 from telo-
meres modifies telomeric organization, we note that the
subtelomeric hybridization is subtly altered in the *sir* mu-
tants, although the lack of Sir3p or Sir4p does not result in
a dispersion of telomeres throughout the nucleoplasm.

Materials and Methods

Yeast Strains and Media

The congenic diploid strains GA192 (*MATa/MATα, ade2-1/ADE2, trp1-
1/TRP1, his3-11,15/his3, ura3-1/ura3-52, leu2-3,112/LEU2, LYS2/lys2-6,
can1-100/CAN1, sir3::TRP1/sir3::LYS2*), GA202 (*MATa/MATα, ade2-1/
ADE2, trp1-1/trp1, his3-11,15/his3, ura3-1/ura3-52, leu2-3,112/LEU2, lys2-
6/LYS2, can1-100/CAN1, sir4::HIS3/sir4::HIS3*), and GA225 (*MATa/
MATα, ade2-1/ADE2, trp1/trp1, his3-11,15/his3, ura3-1/ura3-52, can1-100/
can1-100*) were described in Palladino et al. (1993a). An unrelated Sir⁺
diploid strain was also used where indicated (RS453, described in Doye et
al., 1994). For protein isolation the haploid BJ2168 (*MATa, trp1, ura3-52,
leu2, pep4-3, prb1-1122, prc1-407, gal2*), and the same strain with a com-
plete *sir3::TRP1* disruption (*sir3⁻*; GA421) or a *sir4::LEU2* disruption
(*sir4⁻*; a gift of David Shore, University of Geneva, Switzerland) were
used. The *sir3::TRP1, sir3::LYS2* and *sir4::HIS3* alleles have been de-
scribed elsewhere (Stone et al., 1991; Kimmerly and Rine, 1987). In all of
these *sir* mutant strains silencing is abolished, and for simplicity, they are
referred in the text as *sir3⁻* and *sir4⁻*, respectively. Standard genetic tech-
niques and YPD medium supplemented with 40 mg/l adenine were used
throughout (Rose et al., 1990).

Protein Techniques

For protein blots, crude nuclei from protease deficient strains were pre-
pared as described by Verdier et al. (1990). After incubation in digestion
buffer (10% glycerol, 50 mM NaCl, 20 mM Tris-HCl, pH 6.8, 5 mM
$MgCl_2$, 0.1% Trasylol [Bayer, aprotinin], 1 mM phenylmethylsulfonyl flu-
oride, 1 μg/ml pepstatin, 1 μg/ml leupeptin, 0.05 mg/ml DNase I) for 2 h at
4°C, nuclei were dissociated in sample buffer (Laemmli, 1970). After SDS
gel electrophoresis in 8% polyacrylamide gels, the proteins were Western
blotted by standard techniques with affinity-purified Rap1, Sir3p, and
Sir4p antibodies and peroxidase-coupled goat anti-rabbit Ig (Sigma
Chem. Co., St. Louis, MO). The secondary antibody was detected by En-
hanced ChemiLuminescence (Amersham Corp., Arlington Heights, IL),
and multiple exposures were made for each blot to ensure that the signal
was in a linear range.

Antibody Production, Affinity Purification, and Specificity

The preparation of the rabbit antisera against Rap1 (Klein et al., 1992)
and the full-length Sir3-βgal fusion (Cockell et al., 1995) were previously
described. The anti-Sir4p antibody was raised against the carboxy-termi-

nal 519 aa of the Sir4p protein expressed as a glutathione-S-transferase (GST) fusion protein in *E. coli* (in pGEX, Pharmacia, Dubendorf, Switzerland). Standard immunological methods were used (Harlow and Lane, 1988). All antibodies were affinity purified before use (Gasser et al., 1986), against the following *E. coli* expressed fusion proteins. For Rap1, aa 19-827 of Rap1 were fused to phage T7 gene 10 protein (Gilson et al., 1993), and for anti-Sir antibodies full-length *lacZ-SIR3* and *lacZ-SIR4* fusions were used (Palladino et al., 1993a).

The specificities of the purified anti-Sir3p and anti-Sir4p antibodies were demonstrated by Western blot and immunofluorescence on strains lacking the protein in question. As previously demonstrated with other anti-Sir4p antisera (Palladino et al., 1993a), anti-Sir4p signal migrates around $M_r = 170,000$ in a Sir$^+$ strain (Fig. 1, lanes *13–16*), and is absent in the strain carrying a *sir4* gene disruption (Fig. 1, lanes *17–18*). The affinity-purified anti-Sir3p antibody reacts with two polypeptides in both Sir$^+$ and *sir4*$^-$ strains, one of $M_r = 120,000$ and a more weakly reacting band of $M_r = 116,000$ (Fig. 1, lanes *7–12*). The larger polypeptide is absent in the *sir3::TRP1* strain (Fig. 1, lanes *9–10*). The smaller, more weakly cross-reacting band and several breakdown products do not appear to be derived from the *SIR3* gene, as they are present in extracts of the *sir3* deletion strain (Fig. 1, lanes *9–10*). Although visible on Western blot, the cross-reaction contributes only a weak background immunofluorescence in a *sir3*$^-$ strain (see Fig. 2 *e*); in view of the extensive homology between Sir3p and Orc1, the ~120-kD subunit of the origin recognition complex (Bell et al., 1995), this cross-reacting band is probably the product of the *ORC1* gene.

In all strains tested, the affinity-purified anti-Rap1 recognizes a doublet migrating at $M_r = 116,000$ (Fig. 1, lanes *1–6*), of which the upper band appears to be a hyperphosphorylated form of Rap1. We have previously shown that the anti-Rap1 interaction is competed by an excess of full-length bacterially expressed Rap1 protein both on blots and in immunofluorescence (Klein et al., 1992). All other antibodies were purchased as follows: anti-p62 monoclonal antibody (mAb414; Berkeley Antibody Corp., Berkeley, CA), Texas red–conjugated secondary antibody (Jackson Immunoresearch Labs., West Grove, PA), Cy5-coupled reagents (Milan Analytica, La Roche, Switzerland), and fluorescein-derivatized sheep anti-digoxigenin (DIG) F(ab) fragments (Boehringer Mannheim Corp., Indianapolis, IN). Secondary antibodies are preadsorbed against fixed yeast spheroplasts before use, and no cross-reactivity among these reagents has been detected.

In Situ Hybridization Probes

A 4.8-kb EcoRI/HindIII fragment containing the conserved core of the short (5.4-kb) Y' element was used for in situ hybridization, and was isolated from plasmid pEL42H10 kindly provided by E.J. Louis (Oxford University, Oxford, UK) (see Fig. 4). This probe extends from the middle of one Y' into the middle of an adjacent Y' element, spanning an inter-Y' TG_{1-3} repeat and recognizes all classes of Y' elements. Both the subtelomeric X element, which has a very small "core X" domain of 500 bp that is highly conserved (Louis et al., 1994), and the TG_{1-3} repeat alone (which recognizes 300 bp at every telomere end) hybridize less efficiently than the Y' element. The probe called *LYS2* consist of the 4.85-kb SalI fragment containing *LYS2* from pDP6 (Fleig et al., 1986), and 13 kb of adjacent DNA on Chr. II produced by PCR with appropriate primers. Probes for FISH are labeled by nick-translation (GibcoBRL BioNick System, Basel, Switzerland), using digoxigenin-derivatized dUTP (Boehringer Mannheim Corp.).

To estimate the number of telomeres carrying Y' elements in the two strain backgrounds studied here (GA225 and RS453), we used the 4.8-kb Y' probe to blot a pulsed field gel on which chromosomes of the two strains were separated (a gift of E.J. Louis). In both strains only two pairs of homologues completely lacked the Y' element (i.e., 8 of 64 telomeres). In both strains band intensities suggest that for two other chromosomes, either one homologue or one chromosomal end lacks Y' elements, allowing estimation of the maximum number of Y'-free ends as 10 or 16% (data not shown).

A second determination of Y' element lacking telomeres was by Southern blot analysis of genomic DNA digested with restriction enzymes that do not cut within the Y' sequence (PvuII, SmaI, ApaI, NsiI; Louis and Haber, 1992). Probing with the 4.8-kb Y' sequence revealed a minimum of 13 bands, several of which represent multiple telomeres, as judged by both the size and intensity of the signals. Reprobing with $(TG_{1-3})_n$ and quantifying both sets of signals showed that in GA225, 83% of the $(TG_{1-3})_n$ signal coincided with Y' containing bands, while only 17% was found in short fragments lacking Y' repeats; in RS453, 4% of $(TG_{1-3})_n$ hybridization signal did not coincide with Y' repeats.

Combined Immunofluorescence and In Situ Hybridization on Yeast Cells

Cells were grown overnight to ~1–2 × 10^7 cells/ml and were treated with 1,000 U/ml β-glucanase (lyticase, see Verdier et al., 1990) and 0.1 mg/ml Zymolyase (20T, Seikagaku Corporation, Tokyo, Japan) for 10–12 min at 30°C in YPD medium plus 1.1 M sorbitol (YPD-S). The cells were not fully converted to spheroplasts, but retained part of their cell wall, which appears to help stabilize three-dimensional structure. Cells were washed twice in YPD-S and fixed for 20 min by incubation with 3.7% freshly dissolved formaldehyde in YPD-S. Cells were recovered by centrifugation (1,000 *g* for 5 min), washed three times in YPD-S, spotted on slides and left to air dry for 5 min. Slides were immersed in methanol (6 min) and in acetone (30 s) at −20°C. After rinsing in phosphate-buffered saline containing 0.1% Triton X-100 (PBS-T) and 1% ovalbumin, slides were incubated overnight at 4°C with the affinity-purified antibody diluted 1:2 in PBS-T. Slides were then washed in PBS-T and incubated with the appropriate secondary antibody diluted to 0.025 mg/ml in PBS-T at 37°C for 1 h.

In control studies we have also performed formaldehyde fixation (3.7% in YPD for 20 min at 30°C) before cell wall digestion as described above. This resulted in an identical pattern of anti-Rap1 staining (data not shown), ruling out the possibility that spheroplasting before fixation induces the focal staining pattern. Although this protocol works for immunofluorescence alone, double IF/ FISH labeling on prefixed cells was unsuccessful.

To perform in situ hybridization after IF, slides were fixed again in PBS containing 3.7% freshly dissolved formaldehyde for 20 min and incubated overnight in 4 × SSC (Sambrook et al., 1989), 0.1% Tween 20, 20 μg/ml of preboiled RNaseA at room temperature. The slides were then washed in water, sequentially immersed for 1 min in 70%, 80%, 90%, and 100% ethanol at −20°C, and air dried. After a 5-min denaturation at 72°C in the presence of 70% formamide and 2 × SSC, slides were again immersed for 1 min sequentially in 70%, 80%, 90%, and 100% ethanol at −20°C, and air dried. The hybridization solution (50% formamide, 10% dextran sulfate, 2 × SSC, 0.05 mg/ml labeled probe, and 0.2 mg/ml single-stranded salmon sperm DNA) was applied. After 10 min at 72°C, the slides were incubated 40–50 h at 37°C and washed twice in 0.05 × SSC, once in BT buffer (0.15 M $NaHCO_3$, 0.1% Tween 20, pH 7.5; Scherthan et al., 1994) with 0.05% BSA, and immunodetection was performed in BT buffer with fluorescein-conjugated sheep anti-DIG F(ab) (Boehringer Mannheim) and the Texas red–conjugated goat-anti-rabbit IgG (to refresh immunofluorescence) diluted as described above, for 1 h at 37°C in a humid chamber. After three washes in BT buffer, slides were mounted in 1 × PBS, 50% glycerol, 24 μg/ml 1,4 diazabicyclo-2,2,2,octane, pH 7.5, with 1 μg/ml EtBr.

Confocal microscopy was performed on a Zeiss Axiovert 100 microscope (Zeiss Laser Scanning Microscope 410) with a 63 × or 100 × Plan-Apochromat objective (1.4 oil). To detect EtBr and Texas red fluorochromes, a helium laser was filtered at 543 nm, while for the Cy5 fluorochrome the same laser was filtered at 633 nm. An argon laser at 488 nm was used to detect fluorescein fluorochrome. Under standard imaging conditions no signal from one fluorochrome could be detected on the other filter set. Standardized conditions for the pinhole size, for gain and offset (brightness and contrast), were used for image capture, and each image was the average of 16 scans. The subtracted background value (~15% of the maximum signal) is the signal level outside the cells. Image capture and background subtraction were done uniformly on all images to allow direct comparison. The surface topography profiles were analyzed with ImageQuant software v3.3 (Molecular Dynamics, Sunnyvale, CA).

Quantitation of Fluorescent Signals

The calculation of total foci in cells labeled by either anti-Rap1 or Y' FISH alone was performed by scanning eight sequential 0.3-μm focal sections with separate traces indicating the boundary of the specific labeling (anti-Rap1 or Y' FISH) and of the EtBr-stained nuclear DNA. The spots per nuclear section were summed to give a total per nucleus. Signals that were clearly contiguous from one plane to the next were considered as one focus. The resolution in the Z-axis is lower than in the X-Y plane, which could contribute to an underestimation of foci, due to the apparent fusion of foci from plane to plane.

Quantitation of colocalization between antibody and FISH or anti-pore signals were carried out on computer graphic representations of the fluorescent signals from one focal section taken as near as possible to the equator of the field of cells (see Fig. 6). The threshold for contour tracing

using Adobe Photoshop v3.0 software was set at the value of 140 out of a gray scale maximum of 255, after a normalization of each filter channel independently to give the same maximum signal. This ensures that we analyze colocalization of only the strongest sites of staining, although it can also result in the loss of some less intense foci (see Fig. 6, *arrows*). Texas red (indicating anti-Sir3p, -Sir4p, or -Rap1 antibody) and fluorescein (Y' FISH) signals were printed as red or blue boundary traces, respectively. Three persons independently scored for 50% or more overlap of blue and red traced areas, which was called colocalization. In the case of Sir proteins and Rap1 overlap with Y', there were very few borderline cases. Of the 371 cells analyzed, 15% were labeled by only IF or only FISH, and thus could not be used for analysis. In general we observe that the efficiency of Y' FISH is lower when performed after an immune reaction, and particularly after Sir3p or Sir4p immunostaining, e.g., on a given midsection plane we observe on average only 2.1 Y' foci per nucleus after anti-Sir4p staining, which is only half the average number of Sir4p foci. Therefore, we calculated the percentage of Y' FISH coinciding with anti-Sir4p IF (see Table I), rather than the converse. In the case of Rap1, there is less interference between antibody and Y' FISH, and equal numbers of Rap1 and Y' foci are detected per cell, of which overall 76% of IF signals coincide with Y' FISH, and 73% of FISH signals coincide with Rap1. In the case of Sir3p, 65% of the IF signals coincide with FISH, while 54% of FISH signals coincide with Sir3p signals. The fact that the values are lower for Sir3p appears to reflect a drop in the number of Sir3p foci detected before and after FISH, probably due to a lower avidity of this antibody-antigen complex under FISH conditions. The coincidence of anti-p62 (nuclear pore) with anti-Rap1 was calculated in a similar fashion, screening 70 cells containing 301 Rap1 foci.

The calculation of the frequency of at least 50% surface overlap of a given number of randomly distributed spots (of either 0.2 μm or 0.25 μm in diameter) within a circle (nucleus) of 2 μm in diameter was performed on a SUN computer. The number of red or blue spots was set by a Poisson distribution around a given number (2, 3, or 4), and their positions within the circle were generated randomly. The overlap criterion was tested on all red-blue combinations, in 10^4 simulations, and the percentage of red circles that colocalize with at least one blue circle was recorded. The results of four such simulations were averaged for each combination of numbers.

Results

Antisera were raised against the yeast nuclear proteins Rap1 (Klein et al., 1992), Sir3p, and Sir4p, and antigen-specific immunoglobulins were purified by binding and release from antigen saturated strips of nitrocellulose before use for immunofluorescence or Western blots (see Materi-

als and Methods). Western blot analysis on $sir3^-$ and $sir4^-$ strains indicates the loss of the major reactive bands at roughly $M_r = 120,000$ for Sir3p and $M_r = 170,000$ for Sir4p, in the appropriate mutants (Fig. 1, see Materials and Methods). The lower bands in the anti-Sir3p blot do not derive from the *SIR3* gene; this binding is apparently of low affinity, as this cross-reaction does not contribute a significant background signal in immunofluorescence in a $sir3^-$ strain (see Fig. 2 *e*). The affinity-purified anti-Rap1 recognizes a doublet migrating at $M_r = 116,000$ (Fig. 1, lanes *1–6*), which is efficiently competed by an excess of full-length bacterially expressed Rap1 protein both on blots and in immunofluorescence (Klein et al., 1992).

On the autoradiographs shown in Fig. 1, each pair of lanes corresponds to two levels of loading of the nuclear proteins from each indicated strain (see figure legend) and serial exposures of the Western blots confirmed that the signals were in the linear range of the dose response. The blot suggests that Rap1 levels do not to vary more than twofold in $sir3^-$ and $sir4^-$ strains (Fig. 1, lanes *1–6*), and that the Sir3p protein level is also maintained within this range in the absence of Sir4p, and vice versa (Fig. 1, lanes *7–16*).

Integrity and Three-Dimensional Structure of the Nuclei Are Maintained through the Immunofluorescence Procedure

Immunofluorescence studies revealed strong anti-Rap1 signals at each chromosomal end in spreads of pachytene-stage yeast cells and a limited number of brightly staining foci in vegetatively growing yeast cells (Klein et al., 1992, Palladino et al., 1993a). Immunofluorescence using antibodies against Sir3p or Sir4p showed punctate staining patterns, similar to that observed for Rap1, while anti-topoisomerase II stained nuclear DNA uniformly (Palladino et al., 1993a). The protocol used in all these experiments involves digestion of the cell wall before formaldehyde fixation (see Materials and Methods), although fixing the cells before cell wall digestion results in a similar clustered
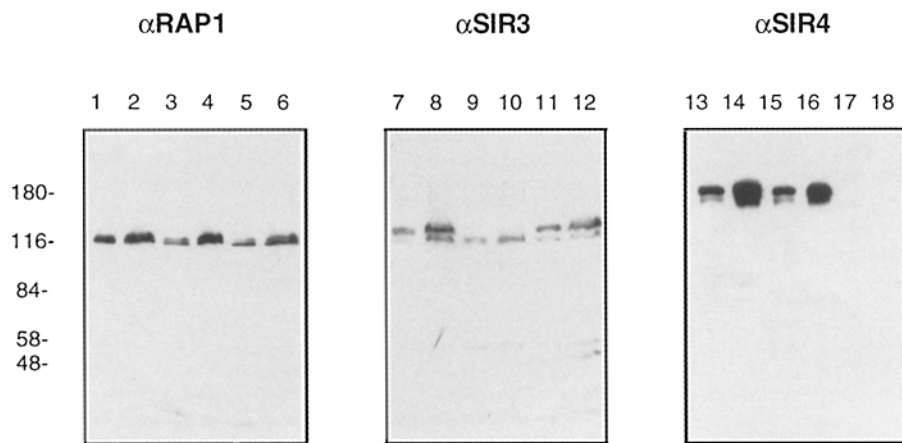

Figure 1. Analysis of affinity purified anti-Rap1, anti-Sir3p and anti-Sir4p antibodies by Western blot. Crude nuclear proteins were isolated from a Sir+ strain, BJ2168, and from strains carrying a *sir3::TRP1* deletion, or a *sir4:: LEU2* disruption. Two lanes of each indicated strain were loaded with either 100 or 200 μg of a nuclear-enriched fraction (Sir+, *1–2, 7–8, 13–14*; sir3-, *3–4, 9–10, 15–16*; and sir4-, *5–6, 11–12, 17–18*). After SDS gel electrophoresis, proteins were transferred to nitrocellulose and probed with affinity purified anti-Rap1 (*1–6*), anti-Sir3p (*7–12*) or anti-Sir4p (*13–18*) antibodies. Secondary antibodies were visualized by Enhanced ChemiLuminescence (Amersham), and various exposures were made to ensure that the peroxidase reaction shown was in a linear range. Sir3p migrates with a M_r around 120,000. The band at 110,000 and the lower breakdown products in lanes *7–12* appear not to be specific for *SIR3*. Although this cross-reaction is visible by blotting techniques, its contribution to immunostaining in a *sir3* deletion strain is minimal (see Fig. 2 *e*). Both Sir3p and Sir4p ($M_r = 170,000$) migrate slightly more slowly than expected from their predicted molecular masses. Markers (in kilodaltons) are indicated at the left.

appearance of Rap1 staining (data not shown). The spheroplasted yeast cells maintain their spherical shape throughout the labeling procedure, as shown by three-dimensional reconstitution of the cell nucleus from a series of focal sections (Palladino et al., 1993a). Dimensions of the nucleus calculated from EtBr fluorescence give a diameter of 2.0 ± 0.2 μm in the XY plane, and 2.4 ± 0.2 μm in the Z axis. This 20% distortion along the Z axis is also observed when cells are fixed before spheroplasting and reflects an integral Z-stretch function of the confocal microscope used. Thus, the spheroplasting technique does not alter the shape of the yeast nucleus. On the other hand, if cells are treated with detergents before fixation, or if spheroplasts are protease-treated before FISH, cells become flattened, no longer maintaining this spherical shape (see Palladino et al., 1993b; Guacci et al., 1994) and the number of Z-sections possible is reduced.

As an independent assay for nuclear integrity, we used a mouse monoclonal antibody raised against the human nuclear pore protein p62, a homologue of yeast Nsp1p (Wimmer et al., 1992). Immunofluorescence of Nsp1p shows a ringlike staining at the nuclear periphery typical of nuclear pore staining and identical to our reactions with anti-p62 (Figs. 2 and 3). In our staining protocol, this staining is lost if cells are spheroplasted to completion before formaldehyde fixation, or if the nuclear envelope is disrupted by detergents (data not shown). This confirms that the presence of a punctate/ringlike staining with anti-p62 correlates with a degree of nuclear integrity. In addition, this antibody allows us to monitor the relationship of the immunofluorescent foci to the nuclear periphery as defined by the nuclear pore signal.

Fig. 2 shows that anti-Rap1, anti-Sir3p, and anti-Sir4p antibodies visualized by a Texas red–conjugated secondary antibody reveal a limited number of brightly staining foci in a wild-type diploid strain (Fig. 2, a, d, and g). Double labeling by addition of the anti-p62 monoclonal antibody attests the nuclear integrity under these immunofluorescence conditions. Quantitation of the coincidence of pore staining with either Rap1 or Sir foci was performed on contour traced images such as those shown in Fig. 3, a and b. Only 13.6% of the Rap1 foci were found to have at least 50% overlap with nuclear pore signals, while 57.1% of the foci were found adjacent to, but having <40% surface overlap with a nuclear pore signal. Thus, while a majority of the Rap1 signal is located near nuclear pores and hence near the nuclear periphery, a very low percentage coincide directly with pore complexes (arrows in Fig. 2, a, d, and g). The "juxtaposition" of Rap1 and pore signals is statistically significant, yet due to the limited resolution of immunofluorescence data, no conclusions can be drawn as to whether or not Rap1 and/or Sir foci directly abut the nuclear envelope.

We next determined the localization of the three proteins in diploid cells deficient for both copies of SIR3 (GA192, Fig. 2, b, e, and h) or SIR4 (GA202, Fig. 2, c, f, and i). The punctate, ringlike nuclear pore staining (detected by a Cy5-conjugated secondary antibody, green in Fig. 2) suggests that nuclear integrity is maintained in both wild-type and mutant cells. As previously shown (Palladino et al., 1993a), Rap1 staining becomes diffuse in sir3⁻ (Fig. 2 b) and sir4⁻ (Fig. 2 c) cells. Here we demonstrate

for the first time that Sir4p staining is also diffuse in sir3⁻ cells (Fig. 2 h), and it is, as expected, absent in a sir4⁻ strain (Fig. 2 i). In sir4⁻ cells, anti-Sir3 staining no longer results in a discrete punctate pattern, but shows one of two morphologies. Either we see a diffuse distribution of Sir3p (data not shown), or we see one or two large, irregularly shaped aggregates (Fig. 2 f), clearly distinguishable from the foci in wild-type cells (Fig. 2 d). It is unclear what this staining pattern represents, but the signals do not coincide with telomeric DNA (data not shown). These double-labeling experiments make it unlikely that the discrete focal patterns of Rap1 and Sir protein staining seen in wild-type cells, and their shift to a diffuse distribution in mutants, reflect either artefacts of the immunofluorescence protocol or loss of nuclear integrity during the assay.

Subtelomeric Hybridization Patterns Reveal Telomere Clusters

Do the staining patterns of Rap1, Sir3p, and Sir4p coincide with telomeres in interphase nuclei? To answer this question, we have combined immunofluorescence and in situ hybridization for the double labeling of S. cerevisiae diploid strains (see Materials and Methods). We aimed to detect both immunofluorescence and in situ hybridization signals, but also to maintain, as much as possible, the three-dimensional organization of the nucleus. For this reason we have omitted the protease treatment usually found in FISH protocols (e.g., Guacci et al., 1994). Attempts to hybridize to the 300-bp TG_{1-3} repeat at the ends of all yeast chromosomes, showed irreproducible labeling efficiency in intact spheroplasts. Therefore, we chose to use the 5.4-kb, highly conserved Y′ subtelomeric element, found immediately adjacent to the terminal TG_{1-3} repeat, as a probe. Although the highly conserved Y′ element is not present at all chromosomal ends due to its strain-dependent distribution (Louis and Haber, 1992), a quantitative screening for the number of Y′-containing telomeres in the two diploid strains used in this study showed that well over 80% of the telomeres have either the 5.4- or the 6.7-kb Y′ element adjacent to the $(TG_{1-3})_n$ repeat (see Materials and Methods; data not shown).

To perform in situ hybridization we adapted the fixation technique that we had optimized for immunofluorescence, knowing that it allows maintenance of the three-dimensional structure of the nucleus as monitored by confocal Z-series analysis. Under these conditions the average diameter of nuclear DNA is unchanged by in situ hybridization (2.0 ± 0.2 μm in the XY plane, and 2.4 ± 0.2 μm in the Z axis), and nuclear pore staining is still detectable after the FISH procedure (Fig. 3, e and f). The average diameter of the nucleus measured after FISH by pore staining is between 2.4 and 2.6 μm, similar to the diameter of nuclear DNA, with an additional 0.2 μm due to the pore signal itself. Fig. 4 shows five 0.3-μm sections of three wild-type yeast nuclei in which the DNA has been stained with ethidium bromide and the telomeres labeled with a Y′ subtelomeric probe, detected by fluorescein-conjugated anti-DIG F(ab) fragments. Because there are 32 chromosomes and 64 telomeres in these cells, of which nearly all contain Y′ repeats (see Materials and Methods), we propose that telomeres are clustered in a limited num-
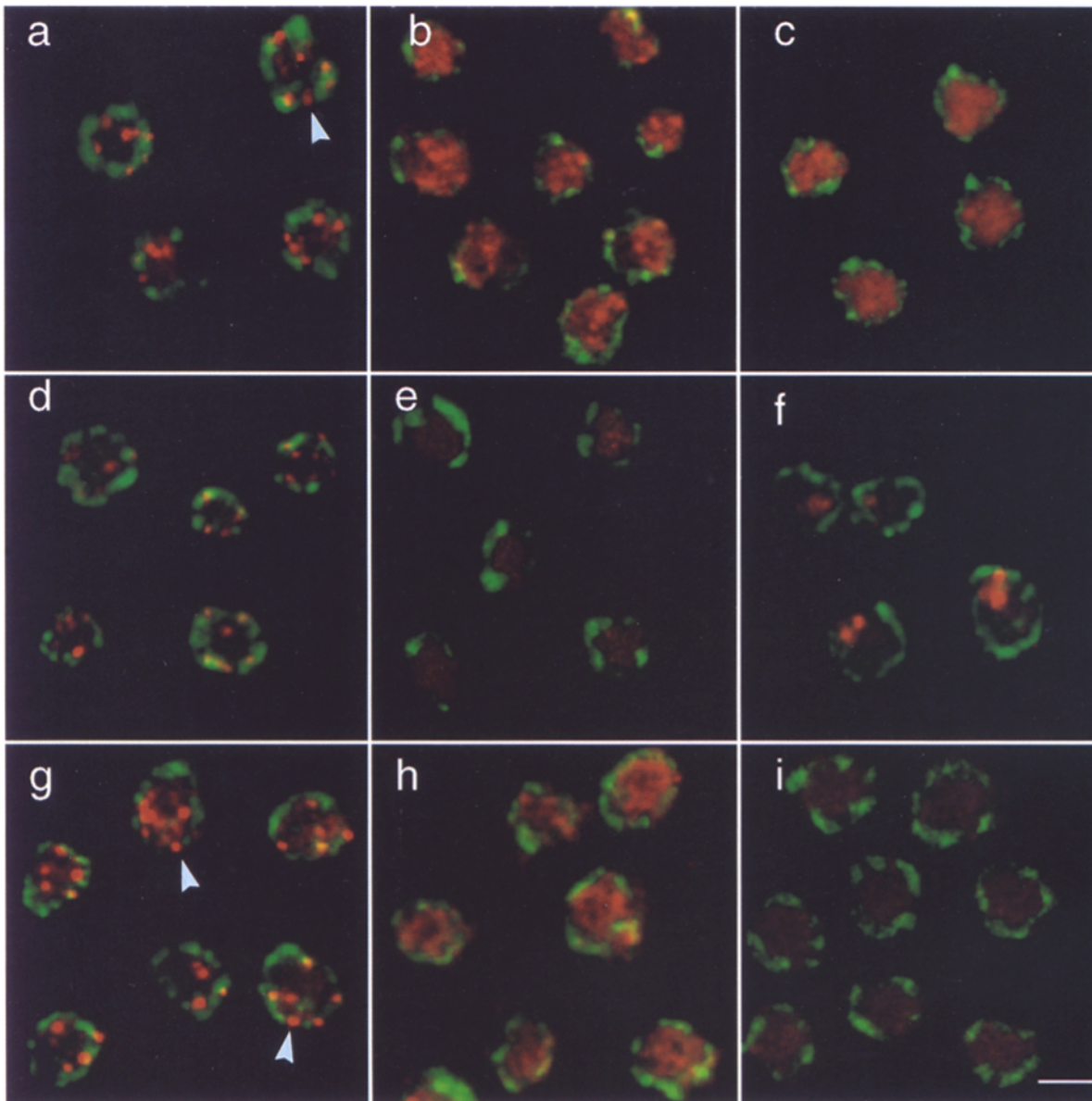
Figure 2. Integrity of nuclei is maintained throughout immunolabeling as monitored by nuclear pore staining. To monitor nuclear integrity after the staining procedure, cells from a Sir$^+$ diploid (RS453, *a, d,* and *g*), a *sir3*$^-$ diploid (GA192, *b, e,* and *h*) and a *sir4*$^-$ diploid (GA202, *c, f,* and *i*) were stained with a mouse anti-p62 antibody detected by a Cy5-conjugated secondary antibody (in *green*), as described in Materials and Methods. Anti-p62 gives the characteristic punctate, ringlike staining in both wild-type and mutant strains. Cells were also stained with anti-Rap1 (*a, b,* and *c*), anti-Sir3p (*d, e,* and *f*), and anti-Sir4p (*g, h,* and *i*) antibodies, visualized as red signals through a Texas red conjugated secondary antibody. Sir3p staining is diffuse or concentrated in a few large regions of staining in *sir4*$^-$ cells (*f*), and is absent, as expected, in *sir3*$^-$ cells (*e*). Sir4p staining is diffuse in *sir3*$^-$ cells (*h*) and absent in *sir4*$^-$ cells (*i*). Shown are images taken on a Zeiss Axiovert 100 LSM confocal microscope using 100× Plan-Apochromat objective. The scanning parameters (pinhole, brightness, and contrast) used were identical for all the images. Bar (*i*) 2 μm. Arrows indicate Rap1 or Sir4p signals adjacent to nuclear pores.

ber of discrete foci, resulting in a staining pattern very similar to that obtained with Rap1, Sir3p, and Sir4p antibodies.

To calculate the total number of Y′ foci in each individual cell, a series of eight 0.3-μm focal sections through four fields of cells was screened so that Y′ foci found in the different focal planes were summed (see Materials and Methods). The number of Y′ foci per nucleus ranged from three to eight, with an average of 5.3 ± 1.3 (*n* = 28; Fig. 5). A similar operation was performed for cells labeled only with anti-Rap1, and we obtained a slightly larger number

of Rap1 foci per nucleus (6.8 ± 1.4; *n* = 24; Fig. 5). This difference is likely to reflect either the reduced efficiency obtained for FISH as compared to immunofluorescence, the fact that two pairs of homologues do not contain Y′ sequences in these strains, or possibly, the presence of Rap1 foci that are not telomeric.

Rap1, Sir3p, and Sir4p Colocalize with Telomeres

Rap1, Sir3p, and Sir4p are essential for telomeric silencing

pore/Rap1
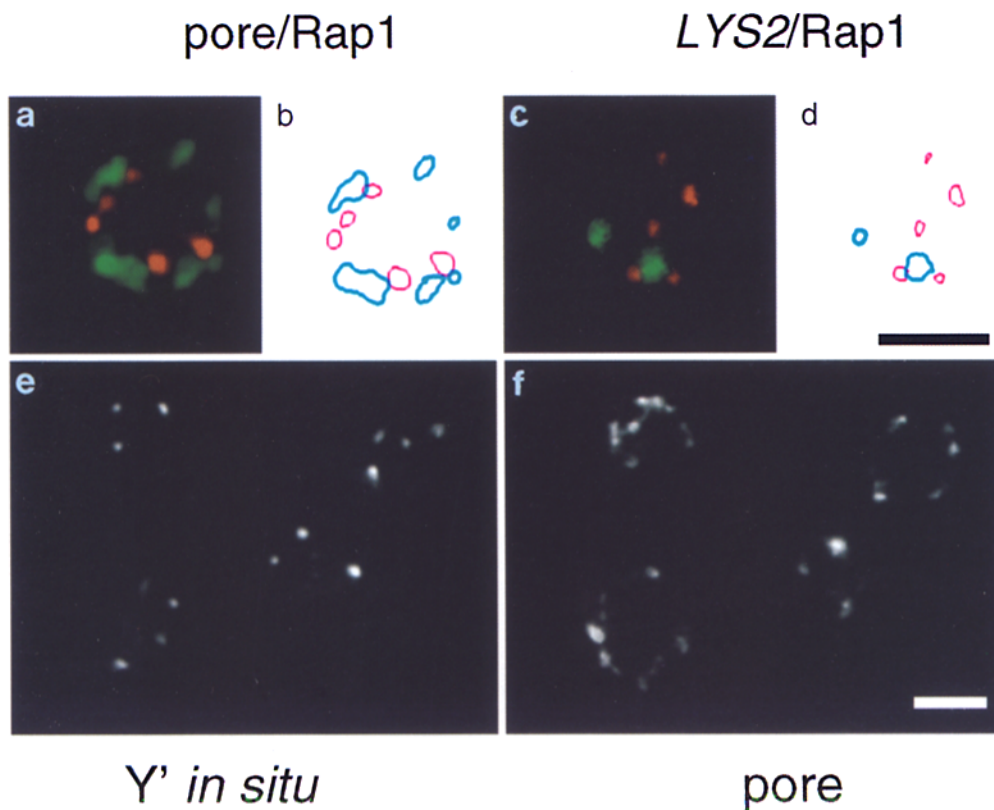
a b

LYS2/Rap1

c d

e f

Y' in situ

pore

Figure 3. Graphic representation of fluorescence signals for nuclear pore/Rap1 and *LYS2/* Rap1 colocalization, and nuclear pore staining on cells subjected to FISH. Shown are representative cells from the double staining for Rap1 (in *red*, *a* and *c*, detected by a Texas red-conjugated secondary antibody) and for nuclear pore (in *green*, *a*, visualized by a Cy5-conjugated secondary antibody), or for *LYS2* FISH (in *green*, *c*, detected by fluorescein-coupled anti-DIG F(ab) fragments). Also shown is the corresponding computer graphic representation (*b* and *d*, *red* for Rap1, *blue* for nuclear pore or *LYS2*, respectively) of signals above a given threshold (see Materials and Methods). Similar traces were used for the quantitation of colocalization. *e* and *f* show Y' FISH (*e*) and nuclear pore staining (*f*) on cells subjected to the double immunofluorescence/ FISH protocol.

(Aparicio et al. 1991; Kyrion et al., 1993), yet Rap1, and possibly Sir proteins, are also involved in other nuclear processes (e.g., Devlin et al., 1991; Gottlieb and Esposito, 1989; Kennedy et al., 1995). It was thus important to ask whether the Rap1, Sir3p, and Sir4p foci coincide with telomeres as detected by in situ hybridization with the Y' probe. To perform combined immunofluorescence with either Rap1, Sir3p, or Sir4p antibodies and in situ hybridization on fixed yeast cells, we perform the standard labeling with affinity-purified Rap1, Sir3p, or Sir4p antibodies, and confirm by fluorescence microscopy that the reaction was successful. The formaldehyde fixation is then repeated, cells are treated with RNaseA and subjected to in situ hybridization. Fig. 6 displays the result of the double-labeling experiment in which Y' in situ hybridization on wild-type cells is detected by fluorescein fluorescence (*a*, *e*, and *i*), while Texas red fluorescence indicates antibody staining (Fig. 6 *b*, anti-Rap1; *f*, anti-Sir3p; and *k*, anti-Sir4p).

A focal staining pattern is obtained with both labeling techniques. To test for colocalization, we merged the two fully independent channels of fluorescence (Fig. 6, *c*, *g*, and *l*). In the merged image, the Y' in situ hybridization is green, the antibody signal red, and coincidence of the most intense signals is indicated in white (see Materials and Methods). Despite the fact that the presence of proteins cross-linked to DNA reduces in situ hybridization efficiency, quantitation of these results confirms a statistically significant colocalization of anti-Rap1, -Sir3p, and -Sir4p staining with Y' telomeric foci (see below).

To quantify the colocalization or direct coincidence of fluorescent signals in each of the combined antibody/

FISH, a graphic representation of the two signals was created directly from the computer using identically scanned images in all cases (see examples Fig. 6, *d*, *h*, and *m*; Materials and Methods). Colocalization was scored on a single focal plane taken as close as possible to the equator of the nucleus, and in each case between 460 and 500 total signals were scored. The results for >50% of surface overlap (defined as colocalization) for foci from Rap1/Y', Sir4p/Y', and Sir3p/Y' labelings are summarized in Table I. For both Rap1- and Sir4p-staining, 73% and 74% of the Y' foci coincide with an antibody signal. In the case of Sir3p, fewer antibody complexes appear to resist the stringent conditions of hybridization (we score on average 1.6 Sir3p foci per nuclear section after FISH, compared to 3.0 foci per nuclear section before FISH), which reduces the chance that a Y' signal can colocalize with a Sir3p focus. The calculated colocalization of Sir3p on Y' is thus 54%, while the frequency with which Sir3p coincides with the Y' signals is 65% (summarized in Table I).

This frequency of signal colocalization could simply reflect a stochastic event due to the small size of the yeast nucleus and the resolution of the signals. To rule out this possibility, we used a nontelomere proximal probe of 13 kb in length, which hybridizes near the *LYS2* locus, 342 kb from the right telomere of Chr. II. The probe gives on average 1.95 signals per diploid nucleus of a signal size roughly equivalent to that obtained with other probes (diameter of 0.2–0.25 μm; see Fig. 3, *c* and *d*). When identical parameters are applied to the images and colocalization of the *LYS2* signal with Rap1 staining is quantified by contour tracing (see Fig. 3, *c* and *d*, Table I), we obtain a value
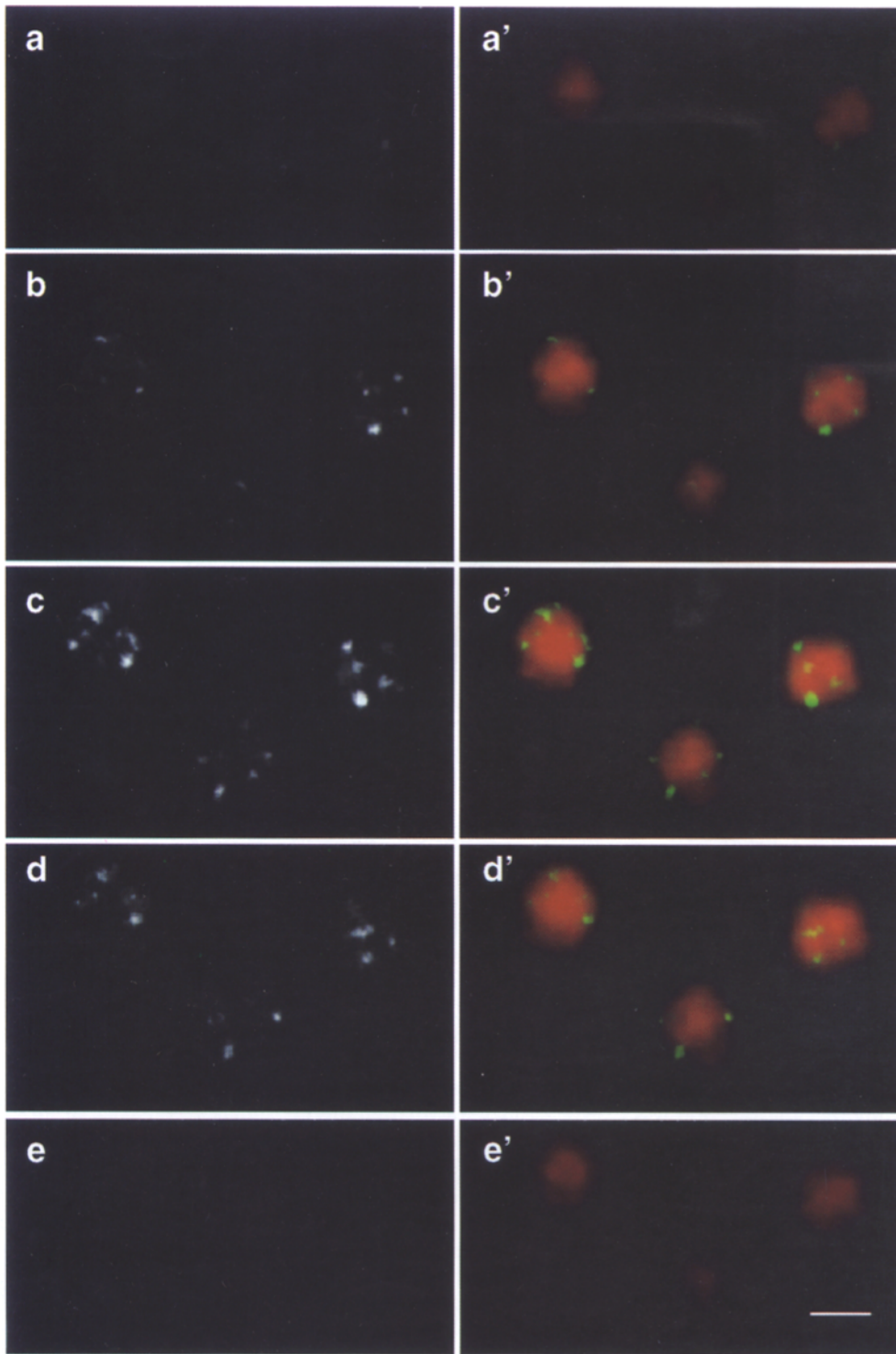
Figure 4. Subtelomeric sequences are found in a limited number of foci. In situ hybridization of yeast diploid cells (RS453) was performed as described in Materials and Methods with a DIG-dUTP labeled Y' sequence which is detected by fluorescein-conjugated anti-DIG F(ab) fragments. *a–e* show the Y' in situ hybridization, *a'–e'* show the merge between the Y' FISH signal and the DNA stained with the ethidium bromide. The five vertical panels show 0.3-μm sections of three fixed yeast cells demonstrating that the three-dimensional structure of the nucleus is maintained after the in situ hybridization. Similar results were obtained with the wild-type strain GA225 (data not shown). At the bottom of the figure is a sketch of the XIIL yeast telomere with two short (~5.4 kb) Y' elements. $(TG_{1-3})_n$ indicates the TG-rich repeat that encompasses ~300 bp at the end of the chromosome and ~60 bp between the two copies of Y'. The position of the probe used is underlined as a HinDIII (H3)-EcoRI (R1) fragment. Bar: (*e*) 2 μm.
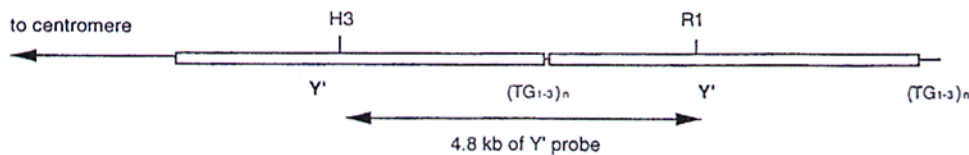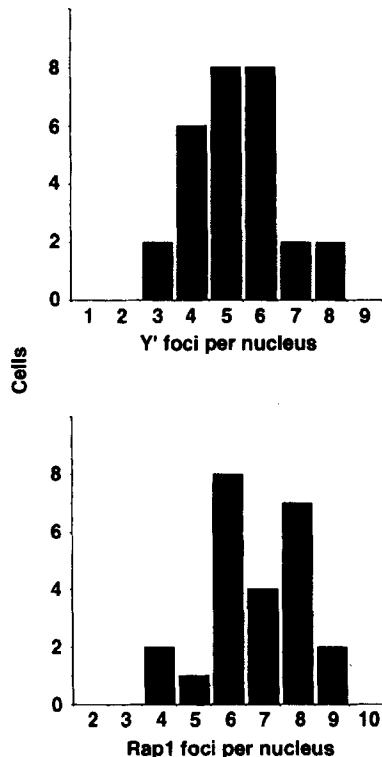
Figure 5. Quantitation of Y' FISH foci and Rap1 foci in yeast nuclei. The wild-type diploid RS453 was labeled with either anti-Rap1 or a DIG-dUTP labeled Y' probe in separate experiments. A series of confocal images such as those shown in Fig. 4 were made on 20 to 25 cells of each labeling. Quantitation of the signals was carried out as described in Materials and Methods on six of the eight 0.3-μm focal sections, since there were no foci in the first and eighth that were not already visible in the adjacent section. The graphs show the distribution of nuclei with respect to their number of either Y' foci (*top*) or Rap1 foci (*bottom*) per nucleus.

of 9% colocalization. The statistical frequency for more than 50% of surface overlap between two circles of 0.25 μm diameter and four other circles of 0.2 μm diameter, randomly distributed in a circle (nuclear section) of 2 μm in diameter, is 9.3% (Table I). For various numbers of 0.2 μm circles representing two classes of signals, randomly distributed on a 2-μm surface, the frequency of overlap varies between 2.6% and 5.8% (as indicated in Table I). This indicates that the frequencies of colocalization observed for Rap1 and Sir foci with Y' signals (54–74%) are highly significant, while the value observed for *LYS2* and Rap1 (9%) would be consistent with chance coincidence.

There are two parameters that reduce the efficiency with which colocalization can be scored. First, the presence of the cross-linked antigen-antibody complex on the subtelomeric domain inhibits the efficiency of hybridization. The second is the threshold set for the contour tracing, which is unlikely to be optimal for all signals. In some cases, foci that are clearly visible by eye are not scored, because the intensity of the signal is below the threshold value used (see example indicated in Fig. 6 *h*). Such highly restrictive threshold values are necessary when scoring colocalization, to avoid meaningless overlap between widely dispersed, low level signals.

Colocalization of Rap1, Sir3p, and Sir4p with Telomeres Is Lost in sir Mutants

What happens to telomeric foci in *sir3* and *sir4* mutants when the silencing complex is disrupted allowing complete derepression of telomere proximal domains? Fig. 7 shows both the Y' in situ on wild-type, *sir3⁻* and *sir4⁻* cells (Fig. 7, *a*, *d*, and *g*), the anti-Rap1 on the same cells (Fig. 7, *b*, *e*, and *h*), and the merge of the two staining patterns (Fig. 7, *c*, *f*, and *i*). Although the Rap1 staining is diffuse in cells lacking Sir3p or Sir4p (7, *e* and *h*), Y' hybridization still appears clustered, and we routinely observe fewer foci than the 54 individual Y'-containing telomeres. Y' FISH in the *sir* mutants analyzed, however, does not have the tightly defined foci observed in wild-type cells and reveals more heterogeneous Y' FISH pattern. In most *sir⁻* cells the hybridization signals appear extended, covering more of the nucleus, although the total fluorescent signal varies less than 10% from strain to strain (see Fig. 7, *d* and *g*). Despite this altered appearance, the Y' signals are not uniformly dispersed through the nucleus like the IF signals for Sir3p, Sir4p, and Rap1 in *sir* mutants (see Fig. 2). The qualitative change in the Y' hybridization signal is also observed when we perform FISH without previous antibody staining (Fig. 8).

To visualize this qualitative difference of the in situ staining pattern, we have used a surface topology program that indicates the intensity at a given site in the cell as a topological peak (Fig. 8). The Y' signals (*g–i* and *d–f* in green) are superimposed on the EtBr-stained DNA (red in *a–f*). The foci in wild-type cells are well defined with high peaks of labeling and distinct valleys between them, while the intensity of Y' foci is lower and more dispersed in *sir* mutants (Fig. 8, *a–c*, see also the horizontal profile), perhaps reflecting a more extended chromatin state for the subtelomeric DNA in *sir⁻* strains. This may reflect its organization in intact cells before the hybridization reaction, yet it could also be produced or exacerbated by the FISH procedure. Since the protocol is identical for both wild-type and mutant cells and the extended Y' pattern is highly reproducible, we favor the interpretation that it reflects a physiological change in subtelomeric organization.

In this context is important to note that the anti-Rap1 staining in *sir3⁻* and *sir4⁻* cells is no longer confined to Y' foci (see Fig. 7). Anti-Rap1 gives a general nuclear staining pattern, neither confined to nor excluded from the telomeric signal. Immunofluorescence alone cannot distinguish between Rap1 being completely diffuse in the nucleus and no longer telomere-bound, or the presence of two populations of Rap1, one telomere-associated and the other diffuse. We favor the latter interpretation because conditions that interfere with Rap1-DNA interaction at telomeres, through either overexpression or mutation of the Rap1 protein, result in chromosome loss rates up 20-fold above wild-type rates (Conrad et al., 1990; Kyrion et al., 1992), while the levels are only 2–5-fold elevated in *sir3* and *sir4* mutant cells (Palladino et al., 1993*a*). Telomere size deregulation events are also much more dramatic in *rap1* mutants, as compared to the modest 50–100 bp loss observed in *sir3* and *sir4* mutants (Conrad et al., 1990; Kyrion et al., 1992; Palladino et al., 1993*a*). Thus, it appears likely that in *sir* mutants, one subpopulation of Rap1 remains telomere-
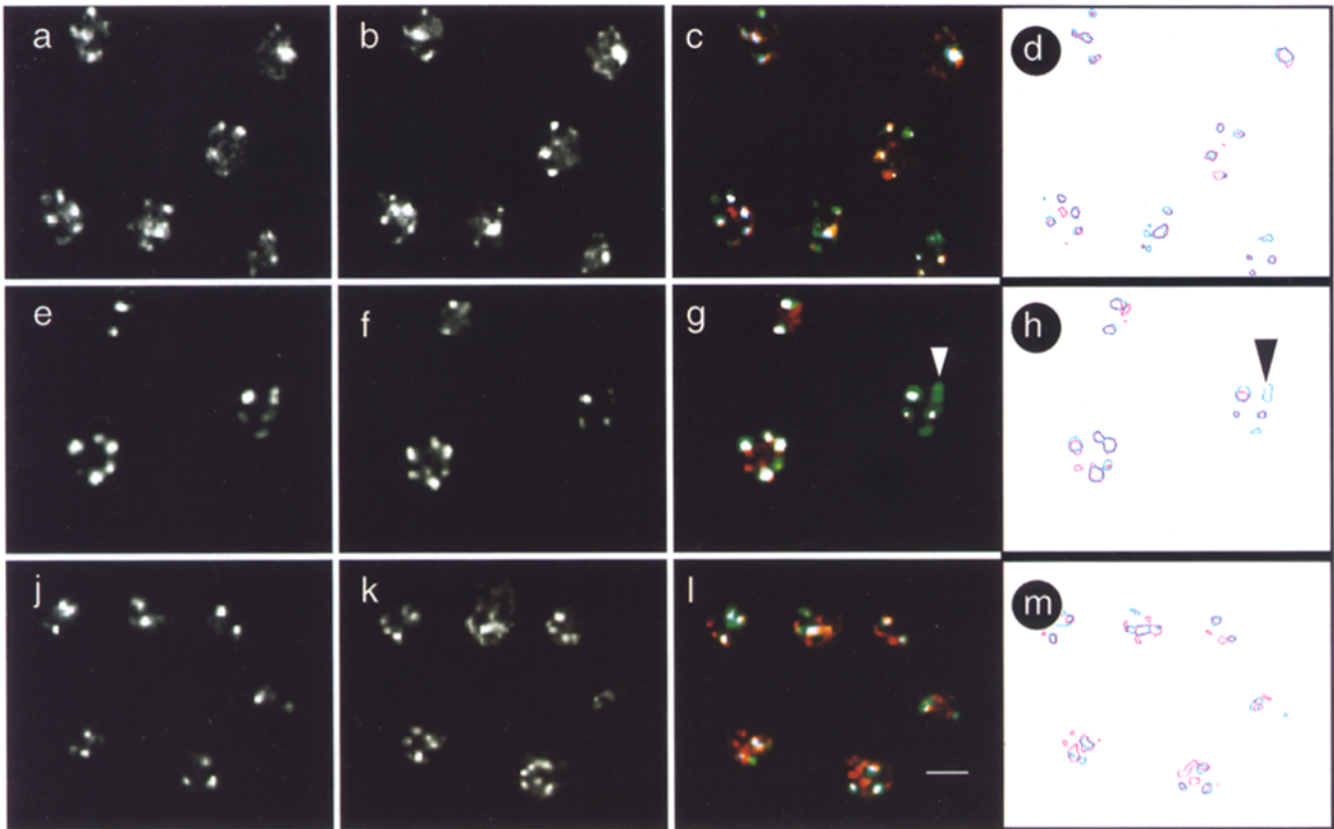
Figure 6. Y' FISH colocalizes with Rap1, Sir3p, and Sir4p foci. The wild-type diploid strain RS453 was subjected to immunofluores-cence with anti-Rap1 (*b*), anti-Sir3p (*f*) and anti-Sir4p (*k*) antibodies which are detected by a Texas red–conjugated secondary antibody; cells were then hybridized with a DIG-dUTP labeled Y' subtelomeric probe (*a, e,* and *j*), detected by a fluorescein-conjugated anti-DIG F(ab) fragment (Materials and Methods). *c* shows the merge of the Rap1 staining (*red*) and the Y' probe (*green*), *g* shows the merge of the Sir3p staining (*red*) and the Y' probe (*green*), and *l* shows the merge of the Sir4p staining (*red*) and the Y' probe (*green*). A single fo-cal section near the equator of the cells is shown. Wave-length shifts are corrected automatically by the Zeiss confocal system. Coinci-dence of the two signals above a given threshold is shown in white (see Materials and Methods). *d, h,* and *m* show the respective com-puter graphic representation of the signals (*red* for the antibody staining, *blue* for the Y' FISH). The treatment of the images for allowing quantitation of colocalization is described in Materials and Methods. The arrows in *g* and *h* indicate an example in which coin-cidence is not scored because the intensity of the Rap1 signal is below the threshold value used, even though the signal is visible. Any weak diffuse nuclear staining of the antibodies is not scored in this procedure. Bar: (*l*) 2 µm.

bound, while another population is released from a telo-meric or subtelomeric complex, producing the general im-munofluorescence pattern visible in Figs. 2 and 7.

Discussion

We have developed a combined immunofluorescence/in situ hybridization protocol for the budding yeast *S. cerevi-siae*, which maintains three-dimensional structure of the nucleus throughout the labeling procedure. We demon-strate by confocal sectioning that the nuclei are not col-lapsed or flattened by the procedure, and that the nuclear pore complexes remain intact at the nuclear periphery. Using the double-labeling technique we demonstrate that Rap1, Sir3p, and Sir4p, three proteins essential for telo-mere proximal gene repression, are indeed localized in foci that correspond to their sites of action at subtelomeric and telomeric domains in wild-type cells. Within the limits of resolution offered by confocal microscopy, we calculate

that over 70% of the Rap1 foci are either adjacent to (57.1%) or coincident with (13.6%) nuclear pore signals, although there is also a significant fraction (29.3%) of Rap1 foci that are more internal in the nucleus. These numbers agree well with a previous analysis of the posi-tioning of Rap1 foci by immunoelectron microscopy (Klein et al., 1992).

The double in situ/immunofluorescence staining proto-col provides a powerful tool for the characterization of nu-clear protein localization and the positioning of specific chromosomal regions. However, by aiming to preserve three-dimensional structure and protein integrity, we also limit the sensitivity of the FISH assay. Short, unique ge-nomic sequences (<10 kb) are difficult to detect reprodu-ibly in our double IF/FISH protocol, although they are quite readily detected in protocols that aim only to opti-mize in situ hybridization (Guacci et al., 1994). There can also be loss of immune complexes during the in situ hy-bridization, although these are minimal when high affinity antibodies (e.g., anti-Rap1) are used.

Table I. Colocalization of FISH and IF Foci

FISH	Y'		LYS2	
IF	Obs	Sim	Obs	Sim
Rap1	73%*	3.9%	9%	9.3%‡
	(3.4; 3.2; 76)	(3; 3; 4 × 10⁴)	(4.1; 2.0; 41)	(4; 2; 4 × 10⁴)
Sir3p	54%§	2.6%	n.d.	n.d.
	(1.6; 1.6; 160)	(2; 2; 4 × 10⁴)		
Sir4p	74%	5.8%	n.d.	n.d.
	(3.6; 2.1; 96)	(4; 2; 4 × 10⁴)		

Shown are the observed (Obs) and computer simulated (Sim) percentages of colocalization between the foci identified by FISH (Y' or LYS2 probes) and the immunofluorescence (IF) signals of Rap1, Sir3p, or Sir4p. The observed colocalization corresponds to the fraction of FISH signals that have a surface overlap of more than 50% with a given IF signal. In parentheses are indicated n, m, and T, where n, the number of IF foci per nuclear plane; m, the number of FISH foci per nuclear plane; and T, the total number of nuclei scored. For the computer simulation, Poisson-distributed numbers of circles ranging from 2 to 4, as indicated in the brackets, were used to calculate the frequency of overlap that would occur by chance in 10^4 nuclei containing two classes of circles in randomly generated positions. For the simulation circles of 0.2 μm diam were used and the nuclear midsection circle was 2 μm in diameter.
*The converse values for the percent of Rap1 foci on Y' spots = 76%.
‡For the simulation of the LYS2 probe, circles of 0.25 μm diam were used, only to demonstrate the effect of slightly larger signals on the chance of colocalization (compare 5.8% with 9.3%). LYS2 signals were not on average larger than Y' signals, however.
§The converse value for the percent Sir3p foci on Y' foci = 65%.

Rap1 Staining Is Coincident with Telomeric DNA in Wild-Type Strains

By combining in situ hybridization, using the highly conserved Y' telomere associated sequence, with anti-Rap1 immunofluorescence, we find colocalization of 74% of the Rap1 foci identified in interphase nuclei of Sir⁺ yeast cells with sites of Y' hybridization, while only 9% of the foci labeled by a single copy internal sequence (LYS2) coincide with Rap1 when analyzed in an identical fashion. 9% is also the percentage of randomly distributed foci that show >50% surface overlap in computer simulation experiments using the same size and number of foci on a surface the size of a yeast nuclear midsection (see Table I). The DNA denaturation required for FISH is somewhat detrimental for the maintenance of the antibody-antigen complex, and depending on the antibody, up to 30% of the immunofluorescence staining can be lost during in situ hybridization. Thus, while the value of 74% colocalization is highly significant, the true value for Rap1 and telomere coincidence is likely to be even higher. Although two pairs of chromosomes in our strains lack Y' elements, and thus escape detection by hybridization, we found that other telomeric probes were less efficient either due to their length (i.e., the terminal TG_{1-3} repeat covers <400 bp) or lack of overall conservation (i.e., only 500 bp core of the X element is highly conserved, Louis et al., 1994). Mixtures of X and Y' probes produce FISH images very similar to those obtained with Y' alone on the strains used in this study (Scherthan, H., T. Laroche, and S.M. Gasser, unpublished results). We cannot, of course, rule out the possibility that a fraction of the Rap1 foci might also reflect aggregates of this protein at sites other than telomeres (e.g., HM loci).

Subtelomeric FISH alone in the absence of anti-Rap1 confirms that telomeres are clustered in a number of foci significantly fewer than the number of chromosomal ends (5.3 detected per average diploid yeast nucleus). We have

also observed using unique telomere probes, that we can detect individual telomeres in these fixed yeast spheroplasts, and that these also colocalize with Rap1 foci (Scherthan, H., and S.M. Gasser, unpublished results). We do not yet know the priniciple of telomere–telomere interaction, nor whether the grouping of telomeres is a stochastic or regulated phenomenon. Ongoing FISH studies with telomere specific probes should provide answers to these questions.

Is There a Nuclear Envelope-Telomere Interaction?

The resolution of light microscopic techniques renders it impossible to judge whether the foci of telomeres, Rap1 or Sir proteins directly abut the nuclear envelope. Roughly 70% of telomeres (or Rap1 foci) have a perinuclear localization, and Rap1 foci do not appear to be directly associated with nuclear pore complexes, since double-immunostaining with anti-Rap1 and anti-pore antibodies show nonoverlapping spots around the nuclear periphery with only 13.6% direct coincidence (Figs. 2 and 3). In addition, we have performed Rap1 immunofluorescence on a strain carrying a mutation in nup133, which provokes the clustering of nuclear pores on one side of the nucleus (Doye et al., 1994). In this strain the Rap1 staining has a wild-type focal pattern, suggesting that Rap1/telomere complexes are positioned independently of the pore complexes (data not shown).

Although it is intriguing that human telomeres associate with the nuclear matrix isolated from cultured cell nuclei (de Lange, 1992), our attempts to purify the yeast nuclear lamina, which might associate with yeast telomeres have failed (see Cardenas et al., 1990; data not shown). Moreover, we show here that despite its coiled-coil domain (Diffley and Stillman, 1989), Sir4 protein does not localize to the nuclear periphery in the absence of Sir3p, nor does it form a perinuclear ring, suggesting that Sir4p alone has no stable link to a peripheral nuclear substructure. If a structural element of the nucleus or a telosome component is responsible for the clustering of telomeres, further studies will be required to identify its components. While telomeres still appear clustered in the nuclei of sir3⁻ or sir4⁻ cells, the resolution of FISH is inadequate to determine whether or not the subnuclear positioning of these clusters is altered in the absence of Sir3p or Sir4p. Other methods of DNA detection with higher resolution will be required to resolve this question.

Sir3p, Sir4p, and a Subpopulation of Rap1 Are Displaced from Telomeres in sir3 and sir4 Mutants

Genetic and biochemical evidence strongly suggest that Rap1, Sir3p, and Sir4p form a multiprotein complex essential for telomeric silencing. Nonsense and missense mutations in the COOH terminus of Rap1 abrogate telomeric repression (Kyrion et al., 1992; Liu et al., 1994) and overexpression of Sir3p suppresses some of these missense mutations (Liu et al., 1994). SIR3 overexpression also suppresses certain sir4 point mutations (Marshall et al., 1987), and two hybrid studies show that domains of Sir3p and Sir4p interact with themselves, with each other, and with Rap1 (Moretti et al., 1994). In addition, full-length Sir4p and Rap1 can be coprecipitated from yeast nuclear ex-
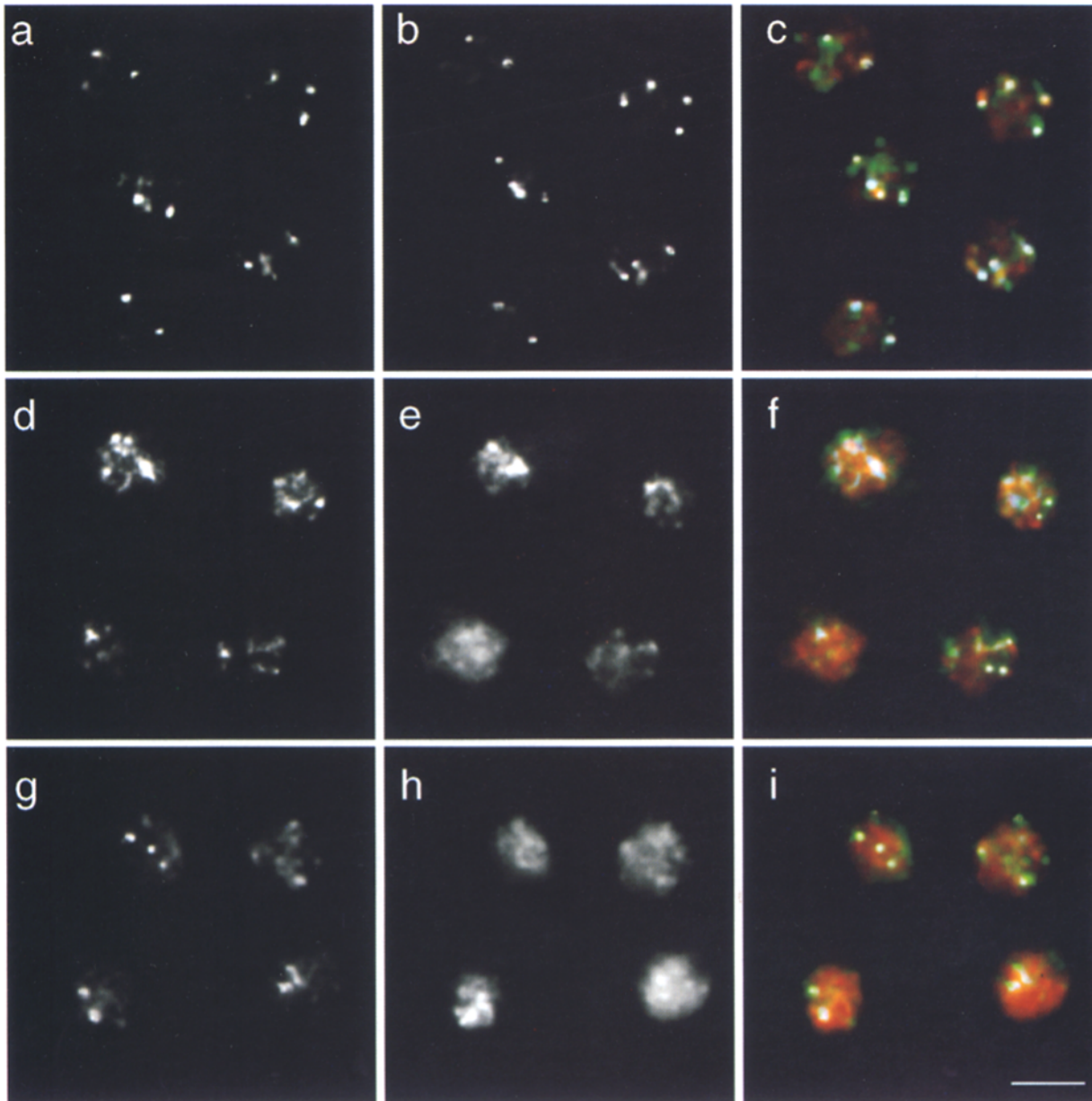
Figure 7. Rap1 staining does not coincide primarily with subtelomeric FISH in *sir3* and *sir4* mutants. Wild-type (RS453, *a–c*), *sir3⁻* (GA192, *d–f*) and *sir4⁻* (GA202, *g–i*) diploid cells were first stained with affinity purified anti-Rap1 antibodies, which are detected by a Texas red–conjugated secondary antibody, and subsequently hybridized with a dig-dUTP labeled Y' probe, detected by fluorescein-coupled anti-DIG F(ab) fragments. *a, d,* and *g* show the FISH signal alone; *b, e,* and *h* show the anti Rap1 staining alone and *c, f,* and *i* show the merge of the FISH and the antibody staining patterns. Rap1 staining is diffuse in mutant strains (*e* and *h*) unlike the Y' probe (*d* and *g*). The total FISH signal integrated over twenty nuclei from each labeling varied <10% among strains. Bar: (*i*) 2 μm.

tracts with either Rap1 or Sir4p antibodies (Cockell et al., 1995). We have shown that Sir3p and Sir4p immunolocalize to a limited number of nuclear foci, much like those identified by anti-Rap1. Here we show unequivocally that Sir3p and Sir4p signals coincide with Y' repeats in wild-type cells, with colocalization values similar to those for Rap1 and Y', all of which are significantly above any stochastic frequencies for overlap (see Table I). This reinforces genetic evidence indicating that these proteins work together in a complex at telomeres.

Evidence that the tertiary complex is necessary for the proper localization of Sir3p, Sir4p, and at least a subpopu-

lation of Rap1, comes from immunofluorescence studies in either *sir3⁻* or *sir4⁻* strains. We see that Rap1 has a general, dispersed nuclear staining in either mutant, while the normal focal pattern of Sir3p becomes diffuse in a *sir4⁻* strain. Likewise, Sir4p staining is diffuse in a *sir3⁻* strain. Because the net signal intensities are not higher in the mutant strains, this result does not reflect the "unmasking" of antigen that was undetected in wild-type cells. We confirm that nuclear integrity is maintained throughout these immunolocalization studies by counter-staining with a monoclonal antibody that recognizes nuclear pores and by confocal Z-series analyses. The somewhat more diffuse Y'
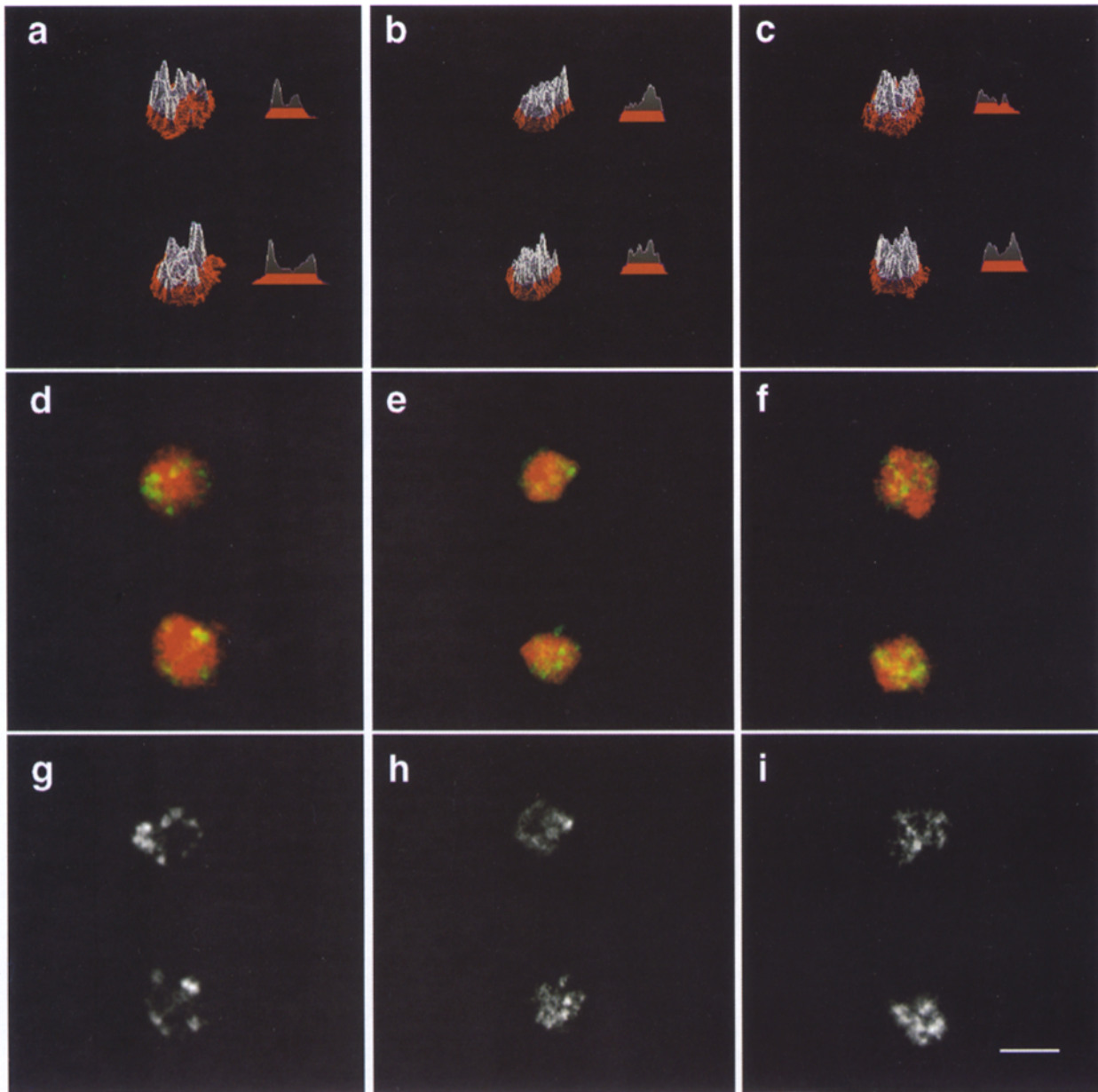
Figure 8. Y' in situ hybridization reveals a qualitatively altered pattern in *sir3* and *sir4* mutants. Shown are surface topography profiles of Y' signal in a focal plane (*top*). Wild-type (RS453, *a, d,* and *g*), *sir3⁻* (GA192, *b, e,* and *h*) and *sir4⁻* (GA202, *c, f,* and *i*) diploid cells were hybridized with a dig-dUTP labeled Y' probe, detected by fluorescein-coupled anti-DIG F(ab) fragments, in the absence of prior antibody staining. Genomic DNA was detected by EtBr staining and is shown in red. A single focal plane containing two cells is shown for each strain, taken from a Z-series analysis which demonstrated three dimensional integrity of the labeled spheroplasts. *d–f* show the merge of the FISH (*green*) and the EtBr stained DNA (*red*), while *g–i* show the FISH image alone. *a–c* show the surface topography profiles of the EtBr-stained DNA (*red*) and the DIG-dUTP FISH labeling (*white*) from the cells shown in *d–f*. The peaks represent the intensity of the signal. A transverse section is also shown for each labeled cell. All representations were calculated with the Carl Zeiss LSM software. The total FISH signal integrated over twenty nuclei from each labeling varied <10% among strains. Bar, 2 μm.

FISH signals in *sir3⁻* and *sir4⁻* cells may reflect an altered, less compact chromatin structure, although other bio-chemical techniques will be required to explore Y' chromatin structure in *sir⁻* strains. More important is the fact that the immunostaining patterns no longer coincide primarily with the Y' signals. This is consistent with our interpretation that the loss of either Sir3p or Sir4p disrupts the proper localization of a Sir3p/Sir4p complex from its normal site of action.

Unexpected was the result that Rap1, which binds its consensus site in vitro with a $K_d = 10^{-11}$ (Vignais et al., 1990), appears dispersed in the Sir-deficient nuclei while telomeres, detected by the telomere associated sequence Y', are still more or less clustered (Fig. 7). Fluorescence techniques are not sensitive enough to differentiate between TG_{1-3} and Y' repeats, hence probing with Y' sequences closely reflects the position of the relatively short TG_{1-} repeat. Our results demonstrate that Rap1 staining is

not sufficient for determining telomere position in mutant strains of *S. cerevisiae*. Because chromosome loss rates are significantly lower in *sir* mutants (Palladino et al., 1993*a*), than in *rap1* mutants (Kyrion et al., 1992), we assume that Rap1 still stabilizes telomeric DNA in *sir*⁻ cells. To account for the dispersed Rap1 staining pattern, we must propose that some fraction of the Rap1 found at telomeric foci in wild-type cells is held there through protein–protein interactions alone. The loss of Sir3p and/or Sir4p displaces this fraction apparently without disrupting telosome function (Sandell and Zakian, 1992). Indeed, proteins other than Sir3p and Sir4p may be involved in the localization of this subpopulation of Rap1, as suggested by Konkel et al. (1995), and these may or may not be involved in conferring repression on telomere proximal genes.

The nonrandom distribution of proteins involved in chromatin-mediated repression is not limited to Sir3p and Sir4p in yeast. Immunostaining has shown an unusual subnuclear distribution of the *Drosophila* Polycomb protein, which, in association with other products of Polycomb-group genes, is responsible for maintaining the repressed state of homeotic genes through development (Paro, 1993). Polycomb shows a punctate pattern of bright spots which is disrupted by mutations in the chromo-domain (Messmer et al., 1992).

Reservoirs or "Sinks" for Silent Information Regulatory Factors

Genetic evidence suggests that a critical local concentration of Sir proteins is necessary to establish or maintain a repressed chromatin state even at internal chromosomal locations (Stavenhagen and Zakian, 1994; Lustig et al., 1996; Maillet et al.,1996; Marcand et al., 1996). We interpret the focal staining pattern we observe by in situ hybridization and immunofluorescence as evidence for a high concentration of Sir3p and Sir4p in the regions of clustered telomeres. Clustered telomeres may be able to create the critical concentration of Sir proteins by providing multiple binding sites for Sir3p and Sir4p through multiple copies of the Rap1 COOH terminus. Consistently, the Sir3p focal staining is lost in *rap1*ᵗ mutants that lose their COOH-terminal Sir3p-binding domain (Cockell et al., 1995). By creating this reservoir of corepressors near telomeres, telomere-bound Rap1 will naturally encouter a Sir complex more frequently than a cotransactivator (Hardy et al., 1992), improving chances that a nearby promoter will be repressed rather than transcribed. Rap1 bound at an internal promoter site, on the other hand, should more readily bind a coactivator than the Sir3p/Sir4p complex, due to the sequestering of Sir3p and Sir4p at telomeres. This compartmentation of interacting factors could thus help bifunctional regulators like Rap1, fulfill their roles as both transcriptional activators and repressors.

A similar, dynamic compartmentation of the nucleus into two transcriptional states was also suggested for *Drosophila*, where genes located in either euchromatin or heterochromatin were shown to need their normal chromosomal environment to be fully functional (for review see Weiler and Wakimoto, 1995). One would expect that disturbance of such distributions might result in a disturbance of the normal transcription pattern. Indeed, a trun-

cated form of Sir4p that affects the protein's subnuclear distribution (Laroche, T., M. Gotta, and B. Kennedy, personal communication) has been recently interpreted in exactly this manner (Kennedy et al., 1995). Further in situ hybridization studies will be able to determine whether nontelomeric repressed domains are associated with a subcompartment of the nucleus, such as that defined by Rap1, Sir3p, and Sir4p staining. We can thus test the hypothesis that such focal staining sites represent functional subdomains of the nucleus.

References

Aparicio, O.M., B.L. Billington, and D.E. Gottschling. 1991. Modifiers of position effect are shared between telomeric and silent mating-type loci in *S. cerevisiae*. *Cell.* 66:1279–1287.

Bell, S.P., J. Mitchell, J. Leber, R. Kobayashi, and B. Stillman. 1995. The multidomain structure of Orc1p reveals similarity to regulators of DNA replication and transcriptional silencing. *Cell.* 83:563–568.

Cardenas, M.E., T. Laroche, and S.M. Gasser. 1990. The composition and morphology of yeast nuclear scaffolds. *J. Cell Sci.* 96:439–450.

Chung, H., C. Shea, S. Fields, R.N. Taub, and L.H.T. Van der Ploeg. 1990. Architectural organization in the interphase nucleus of the protozoan *Trypanosoma brucei*: location of telomeres and mini-chromosomes. *EMBO (Eur. Mol. Biol. Organ.) J.* 9:2611–2619.

Cockell, M., F. Palladino, T. Laroche, G. Kyrion, C. Liu, A.J. Lustig, and S.M. Gasser. 1995. The COOH-termini of Sir4 and Rap1 affect Sir3p localization in yeast cells: evidence for a multicomponent complex required for telomeric silencing. *J. Cell Biol.* 129:909–924.

Conrad, M.N., J.H. Wright, A.J. Wolf, and V.A. Zakian. 1990. Rap1 protein interacts with yeast telomeres *in vivo*: overproduction alters telomere structure and decreases chromosome stability. *Cell.* 63:739–750.

Cremer, T., A. Kurz, R. Zirbel, S. Dietzel, B. Rinke, E. Schröck, M.R. Speicher, U. Mathieu, A. Jauch, P. Emmerich, et al. 1993. The role of chromosome territories in the functional compartmentalization of the cell nucleus. *Cold Spring Harbor Symp. Quant. Biol.* 58:777–792.

de Lange, T. 1992. Human telomeres are attached to the nuclear matrix. *EMBO (Eur. Mol. Biol. Organ.) J.* 11:717–724.

Devlin, C., K. Tice-Baldwin, D. Shore, and K.T. Arndt. 1991. RAP1 is required for BAS1/BAS2- and GCN4-dependent transcription of the yeast *HIS4* gene. *Mol. Cell Biol.* 11:3642–3651.

Diffley, J.F.X., and B. Stillman. 1989. Transcriptional silencing and lamins. *Nature (Lond.).* 342:24

Doye, V., R. Wepf, and E.C. Hurt. 1994. A novel nuclear pore protein Nup133p with distinct roles in poly(A)+ RNA transport and nuclear pore distribution. *EMBO (Eur. Mol. Biol. Organ.) J.* 13:6062–6075.

Ekwall, K., J.-P. Javerzat, A. Lorentz, H. Schmidt, G. Cranston, and R. Allshire. 1995. The chromodomain protein Swi6: a key component at fission yeast centromeres. *Science (Wash. DC).* 269:1429–1431.

Fleig, U.N., R.D. Pridmore, and P. Philippsen. 1986. Construction of *LYS2* cartridges for use in genetic manipulations of *Saccharomyces cerevisiae*. *Gene.* 4:237–245.

Funabiki, H., I. Hagan, S. Uzawa, and M. Yanagida. 1993. Cell cycle-dependent specific positioning and clustering of centromeres and telomeres in fission yeast. *J. Cell Biol.* 121:961–976.

Gasser, S.M., T. Laroche, J. Falquet, E. Boy de la Tour, and U.K. Laemmli. 1986. Meta-phase chromosome structure: involvement of topoisomerase II. *J. Mol. Biol.* 188:613–629.

Gilson, E., and S.M. Gasser. 1995. Repressor activator protein 1 and its ligands: organising chromatin domains. *Nucleic Acids Mol. Biol.* 9:308–327.

Gilson, E., M. Roberge, R. Giraldo, D. Rhodes, and S.M. Gasser. 1993. Distortion of the DNA double helix by Rap1 at silencers and multiple telomeric

binding sites. *J. Mol. Biol.* 231:293–310.

Gottlieb, S., and R.E. Esposito. 1989. A new role for a yeast transcriptional silencer gene, *SIR2*, in regulation of recombination in ribosomal DNA. *Cell.* 56:771–776.

Gottschling, D.E., O.M. Aparacio, B.L. Billington, and V.A. Zakian. 1990. Position effect at *S. cerevisiae* telomeres: reversible repression of Pol II transcription. *Cell.* 63:751–762.

Guacci, V., E. Hogan, and D. Koshland. 1994. Chromosome condensation and sister chromatid pairing in budding yeast. *J. Cell Biol.* 125:517–530.

Hardy, C.F., D. Balderes, and D. Shore. 1992. Dissection of a carboxy-terminal region of the yeast regulatory protein Rap1, with effects on both transcriptional activation and silencing. *Mol. Cell. Biol.* 12:1209–1217.

Harlow, E., and D. Lane. 1988. Antibodies: A Laboratory Manual. Cold Spring Harbor Laboratory Press, Cold Spring Harbor, NY. 725 pp.

Hecht, A., T. Laroche, S. Strahl-Bolsinger, S.M. Gasser, and M. Grunstein. 1995. Histone H3 and H4 N-termini interact with the silent information regulators Sir3p and Sir4p: a molecular model for the formation of heterochromatin in yeast. *Cell.* 80:583–592.

Hochstrasser, M., D. Mathog, Y. Gruenbaum, H. Saumweber, and J. Sedat. 1986. Spatial organization of chromosomes in the salivary gland nuclei of *Drosophila melanogaster. J. Cell Biol.* 102:112–121.

Kennedy, B.K., N.R. Austriaco, J. Zhang, and L. Guarente. 1995. Mutation in the silencing gene *SIR4* can delay aging in *S. cerevisiae. Cell.* 80:485–496.

Kimmerly, W.J., and J. Rine. 1987. Replication and segregation of plasmids containing *cis*-acting regulatory sites of silent mating-type genes in *Saccharomyces cerevisiae* are controlled by the *SIR* genes. *Mol. Cell. Biol.* 7:4225–4237.

Klein, F., T. Laroche, M.E. Cardenas, J.F.-X. Hofmann, D. Schweizer, and S.M. Gasser. 1992. Localization of Rap1 and topoisomerase II in nuclei and meiotic chromosomes of yeast. *J. Cell. Biol.* 117:935–948.

Konkel, L.M.C., S. Enomoto, E.M. Chamberlain, P. McCune-Zierath, S.J.P. Iyadurai, and J. Berman. 1995. A class of single-stranded telomeric DNA-binding proteins required for Rap1p localization in yeast nuclei. *Proc. Natl. Acad. Sci. USA.* 92:5558–5562.

Kyrion, G., K.E. Boakye, and A.J. Lustig. 1992. C-terminal truncation of RAP1 results in the deregulation of telomere size, stability, and function in *Saccharomyces cerevisiae. Mol. Cell. Biol.* 12:5159–5173.

Kyrion, G., K. Liu, L. Cheng, and A.J. Lustig. 1993. RAP1 and telomere structure regulate telomere position effects in *Saccharomyces cerevisiae. Genes Dev.* 7:1146–1159.

Laemmli, U.K. 1970. Cleavage of structural proteins during the assembly of the head of bacteriophage T4. *Nature (Lond.).* 227:680–685.

Liu, C., X. Mao, and A.J. Lustig. 1994. Mutational analysis defines a C-terminal tail domain of RAP1 essential for telomeric silencing in *Saccharomyces cerevisiae. Genetics.* 138:1025–1040.

Louis, E.J., and J.E. Haber. 1992. The structure and evolution of subtelomeric Y' repeats in *Saccharomyces cerevisiae. Genetics.* 331:547–574.

Louis, E.J., E.S. Naumova, A. Lee, G. Naumov, and J.E. Haber. 1994. The chromosome end in yeast: its mosaic nature and influence on recombination dynamics. *Genetics.* 136:789–802.

Lundblad, V., and J.W. Szostak. 1989. A mutant with a defect in telomere elongation leads to senescence in yeast. *Cell.* 57:633–643.

Lustig, A.J., S. Kurtz, and D. Shore. 1990. Involvement of the silencer and UAS binding protein RAP1 in regulation of telomere length. *Science (Wash. DC).* 250:549–553.

Lustig, A.J., C. Liu, C. Zhang, and J.P. Hanish. 1996. Tethered Sir3p nucleates silencing at telomeres and internal loci in *Saccharomyces cerevisiae. Mol. Cell Biol.* 16:2483–2495.

Maillet, L., C. Boscheron, M. Gotta, S. Marcand, E. Gilson, and S.M. Gasser. 1996. Evidence for silencing subcompartments within the yeast nucleus: a role for telomere proximity and Sir protein concentration in silencer-mediated repression. *Genes & Dev.* 10: In press.

Marcand, S., P. Moretti, S. Buck, E. Gilson, and D. Shore. 1996. Silencing of genes at non telomeric sites in yeast is controlled by sequestration of silenc-

ing factors at telomeres by Rap1 protein. *Genes & Dev.* 10:1297–1309.

Marshall, M., D. Mahoney, A. Rose, J.B. Hicks, and J.R. Broach. 1987. Functional domains of *SIR4*, a gene required for position effect regulation in *S. cerevisiae. Mol. Cell. Biol.* 7:4441–4452.

Mathog, D., M. Hochstrasser, Y. Gruenbaum, H. Saumweber, and J. Sedat. 1984. Characteristic folding pattern of the polytene chromosomes in *Drosophila* salivary glands nuclei. *Nature (Lond.).* 308:414–421.

Messmer, S., A. Franke, and R. Paro. 1992. Analysis of the functional role of the *Polycomb* chromo domain in *Drosophila melanogaster. Genes Dev.* 6: 1241–1254.

Moretti, P., K. Freeman, L. Coodly, and D. Shore. 1994. Evidence that a complex of SIR proteins interacts with the silencer and telomere binding protein RAP1. *Genes Dev.* 8:2257–2269.

Palladino, F., T. Laroche, E. Gilson, A. Axelrod, L. Pillus, and S. M. Gasser. 1993a. SIR3 and SIR4 proteins are required for the positioning and integrity of yeast telomeres. *Cell.* 75:531–542.

Palladino, F., T. Laroche, E. Gilson, L. Pillus, and S.M. Gasser. 1993b. The positioning of yeast telomeres depends on SIR3, SIR4, and the integrity of the nuclear membrane. *Cold Spring Harbor Symp. Quant. Biol.* 58:733–746.

Paro, R. 1993. Mechanisms of heritable gene repression during development of *Drosophila. Curr. Opin. Cell Biol.* 5:999–1005.

Rabl, C. 1885. Uber Zellteilung. *Morphol. Jahrbuch.* 10:214–230.

Rae, P.M.M., and W.W. Franke. 1972. The interphase distribution of satellite DNA-containing heterochromatin in mouse nuclei. *Chromosoma.* 39:443–456.

Rose, M.D., F. Winston, and P. Hieter. 1990. Methods in Yeast Genetics. Cold Spring Harbor Laboratory Press, Cold Spring Harbor, NY. 198 pp.

Sambrook, J., E.F. Fritsch, and T. Maniatis. 1989. Molecular Cloning. Volumes I–III. Cold Spring Harbor Laboratory, Cold Spring Harbor, NY.

Sandell, L., and V.A. Zakian. 1992. Telomeric position effect in yeast. *Trends Cell Biol.* 2:10–14.

Scherthan, H., T. Cremer, U. Arnason, A. Lima-de-Faria, H.-U. Weier, and L. Frönicke. 1994. Comparative chromosome painting discloses homologous segments in distantly related mammals. *Nature Genet.* 6:342–347.

Shaw, P., M. Highett, and D. Rawlins. 1992. Confocal microscopy and image processing in the study of plant nuclear structure. *J. Microsc.* 166:87–97.

Shore, D., and K. Nasmyth. 1987. Purification and cloning of a DNA binding protein from yeast that binds to both silencer and activator elements. *Cell.* 51:721–732.

Stavenhagen, J.B., and V.A. Zakian. 1994. Internal tracts of telomeric DNA act as silencers in *Saccharomyces cerevisiae. Genes Dev.* 8:1411–1422.

Stone, E.M., M.J. Swanson, A.M. Romeo, J.B. Hicks, and R. Sternglanz. 1991. The *SIR1* gene of *Saccharomyces cerevisiae* and its role as an extragenic suppressor of several mating-defective mutants. *Mol. Cell. Biol.* 11:2253–2262.

Verdier, J.-M., R. Stalder, M. Roberge, B. Amati, A. Sentenac, and S.M. Gasser. 1990. Preparation and characterization of yeast nuclear extracts for efficient RNA polymerase B (II)-dependent transcription *in vitro. Nucleic Acids Res.* 18:7033–7039.

Vignais, M.L., J. Huet, J.M. Buhler, and A. Sentenac. 1990. Contacts between the factor TUF and RPG sequences. *J. Biol. Chem.* 265:14669–14674.

Vourc'h, C.L., D. Taruscio, A.L. Boyle, and D. Ward. 1993. Cell cycle dependent distribution of telomeres, centromeres, and chromosome specific subsatellite domains in the interphase nucleus of mouse lymphocytes. *Exp. Cell Res.* 205:142–151.

Walker, C.L., C.B. Cargile, K.M. Floy, M. Delannoy, and B.R. Migeon. 1991. The Barr body is a looped X chromosome formed by telomere association. *Proc. Natl. Acad. Sci. USA.* 88:6191–9195.

Weiler, S., and B.T. Wakimoto. 1995. Heterochromatin and gene expression in *Drosophila. Annu. Rev. Genet.* 29:577–606.

Wimmer, C., V. Doye, P. Grandi, U. Nehrbass, and E.C. Hurt. 1992. A new subclass of nucleoporins that functionally interact with nuclear pore protein Nsp1. *EMBO (Eur. Mol. Biol. Organ.) J.* 11:5051–5061.

Wright, J.H., D.E. Gottschling, and V.A. Zakian. 1992. *Saccharomyces* telomeres assume a non-nucleosomal chromatin structure. *Genes Dev.* 6:197–210.